Brain Struct Funct
DOI 10.1007/s00429-016-1245-6

SHORT COMMUNICATION

Dorsal and ventral stream contributions to form-from-motion perception in a patient with form-from motion deficit: a case report

Manuel R. Mercier[1,2,3,6] · Sophie Schwartz[4,5] · Laurent Spinelli[3] · Christoph M. Michel[2] · Olaf Blanke[1,3,7]

Received: 24 April 2014 / Accepted: 28 May 2016

Abstract The main model of visual processing in primates proposes an anatomo-functional distinction between the dorsal stream, specialized in spatio-temporal information, and the ventral stream, processing essentially form information. However, these two pathways also communicate to share much visual information. These dorso-ventral interactions have been studied using form-from-motion (FfM) stimuli, revealing that FfM perception first activates dorsal regions (e.g., MT+/V5), followed by successive activations of ventral regions (e.g., LOC). However, relatively little is known about the implications of focal brain damage of visual areas on these dorso-ventral interactions. In the present case report, we investigated the dynamics of dorsal and ventral activations related to FfM perception (using topographical ERP analysis and electrical source imaging) in a patient suffering from a deficit in FfM perception due to right extrastriate brain damage in the ventral stream. Despite the patient's FfM impairment, both successful (observed for the highest level of FfM signal) and absent/failed FfM perception evoked the same temporal sequence of three processing states observed previously in healthy subjects. During the first period, brain source localization revealed cortical activations along the dorsal stream, currently associated with preserved elementary motion processing. During the latter two periods, the patterns of activity differed from normal subjects: activations were observed in the ventral stream (as reported for normal subjects), but also in the dorsal pathway, with the strongest and most sustained activity localized in the parieto-occipital regions. On the other hand, absent/failed FfM perception was characterized by weaker brain activity, restricted to the more lateral regions. This study shows that in the present case report, successful FfM perception, while following the same temporal sequence of processing steps as in normal subjects, evoked different patterns of brain

✉ Olaf Blanke
olaf.blanke@epfl.ch

Manuel R. Mercier
manuel.mercier@a3.epfl.ch

Sophie Schwartz
sophie.schwartz@unige.ch

Laurent Spinelli
laurent.spinelli@hcuge.ch

Christoph M. Michel
christoph.michel@unige.ch

[1] Laboratory of Cognitive Neuroscience, Brain-Mind Institute, Ecole Polytechnique Fédérale de Lausanne (EPFL), Station 19, 1015 Lausanne, Switzerland

[2] The Functional Brain Mapping Laboratory, Department of Neuroscience, University of Geneva, Geneva, Switzerland

[3] Department of Neurology, University Hospital, Geneva, Switzerland

[4] Department of Fundamental Neuroscience, University of Geneva, Geneva, Switzerland

[5] Swiss Center for Affective Sciences, University of Geneva, Geneva, Switzerland

[6] Present Address: Centre de Recherche Cerveau et Cognition (CerCo), CNRS, UMR5549, Pavillon Baudot CHU Purpan, BP 25202, 31052, Toulouse Cedex, France

[7] Laboratory of Cognitive Neuroscience, Center for Neuroprosthetics and Brain Mind Institute, Swiss Federal Institute of Technology (EPFL), Chemin des Mines 9, 1202 Geneva, Switzerland

Published online: 18 June 2016

activity. By revealing a brain circuit involving the most rostral part of the dorsal pathway, this study provides further support for neuro-imaging studies and brain lesion investigations that have suggested the existence of different brain circuits associated with different profiles of interaction between the dorsal and the ventral streams.

Keywords Perceptual deficit · Form-from-motion · EEG · Brain lesion

Introduction

Converging evidence from human and animal data indicate that form and spatiotemporal processing (such as motion perception) are carried out by separate neural pathways in the visual cortex (Mishkin and Ungerleider 1982; Tootell et al. 1996; Goodale and Milner 1992). However, less is known about their functional interactions (Ungerleider and Haxby 1994; Maunsell and Newsome 1987). Also, since different features of a single object in the visual scene (such as its motion, color, or form) are processed by different visual areas, these areas are presumed to communicate for an integrated percept to arise (Tononi et al. 1992; Bullier 2001).

Form stimuli defined by motion (here called form-from-motion, FfM) have been designed and used to study interactions between dorsal and ventral stream processing, as FfM perception requires the integration of visual motion information over time to extract the form (Gulyas et al. 1994; Schoenfeld et al. 2003; Wang et al. 1999; Matheson and McMullen 2010).

Several brain imaging studies have investigated the neural mechanisms of FfM perception. Both positron emission tomography (PET, Gulyas et al. 1994) and functional magnetic resonance imaging (MRI, Wang et al. 1999) have revealed the activation of a large cortical network, including the dorsal (posterior temporal) and ventral regions (inferior and lateral temporo-occipital) of the visual pathway. The temporal dynamics of the activations evoked by FfM perception were studied using magnetoencephalography (MEG, Schoenfeld et al. 2003) and revealed a series of three processing steps: first, activation of area MT+/V5, followed by the lateral occipital cortex (LOC) and finally the inferior temporal cortex (IT). Thus, in the case of FfM perception, dorso-ventral interactions appeared to occur in a sequential manner with, first, involvement of the most lateral regions of the dorsal pathway dedicated to motion processing, followed by activation of ventral brain regions implicated in form processing.

Additionally, neuropsychological studies of perceptual deficits following brain damage have revealed cases of selective FfM blindness (Blanke et al. 2007; Cowey and Vaina 2000; Regan et al. 1992; Schenk and Zihl 1997; Vaina 1989; Gilaie-Dotan et al. 2011; Vaina et al. 2010). In these patients, neither basic motion perception nor static form perception was impaired, suggesting the existence of cortical region(s) and/or anatomical connection(s) dedicated to FfM processing. Diverse brain lesions were linked to FfM selective perception deficit in those studies, either located in ventral regions or in different parts of the dorsal regions, notably in its parieto-occipital part where no FfM-related activations were found in imaging studies. This points to the need for additional investigation to elucidate the anatomo-functional basis of FfM processing. Case studies of patients with fragmentary FfM perceptual deficits following focal brain damage are particularly helpful to clarify the respective contributions of the remaining healthy cortical circuits.

In this study, we combined electrical neuroimaging with neuropsychology to investigate FfM processing in a patient with a specific deficit in FfM perception (i.e., the patient presented normal perception for form and more elementary motion). The deficit was due to predominant ventral stream damage and led to important difficulties in perceiving forms in motion (confirmed by abnormally large perceptual thresholds in FfM perception). Neural mechanisms of FfM processing were investigated using high-density event-related potential (ERP) mapping and source localization for both successful and absent/failed FfM perception. We found that successful FfM perception (observed for high levels of FfM signal) presented an identical temporal sequence of three processing steps as observed in healthy subjects (Schoenfeld et al. 2003), with the first step involving motion specific dorsal regions. Importantly, in contrast to healthy subjects, at the later stages of successful FfM perception strong parieto-occipital activations were found, followed by co-activation in dorsal and ventral regions.

These observations suggest that dorsal and ventral co-activations, with an implication of parieto-occipital cortex, may be associated with an FfM perception deficit caused by right posterior ventral brain damage.

Materials and methods

Experimental procedure

Patient

Twelve months prior to the present FfM experiment, clinical investigations in this left-handed 65-year-old female physician with a history of memory and attention

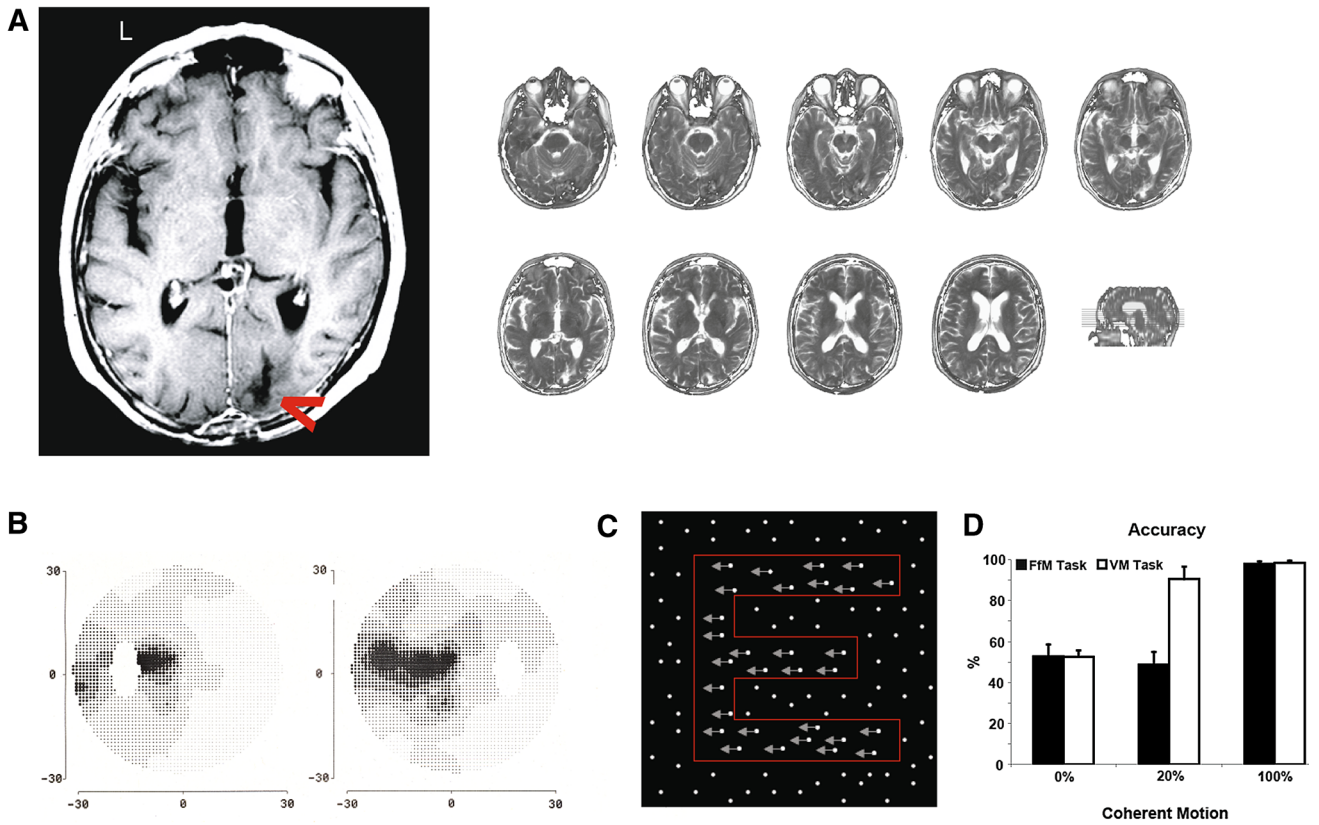

Fig. 1 Neurological and neuropsychological status. **a** Magnetic resonance imaging (T1-MRI with contrast agent) showing the right lateral and medial occipital brain damage extending toward the temporal lobe. Magnified view depicts the MRI slice presenting the largest extent of the lesion (*red arrow*). **b** Visual field testing with computerized perimetry (for left and right eye). *Level of darkness* indicates visual acuity (with *smaller dots* representing 100 % detection accuracy). **c** Stimulus example, with form oriented rightward (e.g., correct response in the FfM task), whereas 100 % of coherent motion is directed to the left (e.g., correct response in VM task). For illustration purpose, the contour is depicted in *red*, and *white arrows* indicate the direction of the dots moving coherently. **d** Behavioral testing results in the FfM task (*black bars*) and the VM task (*white bar*) during the ERP recoding (mean ± standard deviation). Note, her performance is at chance level in the FfM task at 20 % CM, but almost 100 % correct in the VM task, reflecting her deficit compared to controls

deficits revealed the presence of a triventricular hydrocephalus. The condition was due to a pineal cyst located at the floor of the third ventricle. The cyst was eventually resected by a right occipital approach.

Following surgery, the patient noted a left homonymous paracentral scotoma. Computerized perimetry [OCTOPUS 2000R automated perimeter; Interzeag AG, Switzerland; as used in Blanke et al. (2007)] revealed a left homonymous paracentral scotoma located along the horizontal meridian, with preserved visual sensitivity in the fovea and remaining left upper/lower field (Fig. 1b). Follow-up examinations showed good recovery during the following months and stabilization within 4 months post-surgery, with visual acuity returning to normal. Magnetic resonance imaging (MRI) revealed a right lateral and medial occipital hemorrhage extending toward the temporal lobe. The extent of the lesion was re-examined and confirmed during a control MRI examination 12 months post-surgery (Fig. 1a).

Neuropsychological examinations revealed symptoms of memory deficit, spatial disorientation, prosopagnosia (Benton face recognition test), spatial and visual agnosia (Visual Object and Space Perception test). Color perception (Farnsworth 100 hue test) was also moderately impaired, but reading, writing, language, praxis and executive functions were unaltered. The patient, although functionally independent, was still reporting mild difficulties in her daily life for fine visuo-motor coordination and for perception of moving objects.

Assessment of her psychophysical thresholds in visual motion perception and in FfM perception revealed a dissociation: compared with a control group, her visual performance was normal for motion perception (detection of motion direction) and for motion in depth perception, but was severely impaired for FfM perception. This status was considered pathological based on the 99 % prediction intervals calculated for the three tasks, as defined by the routine normed examination used at the Ophthalmology

Department of the Geneva Hospital that is based on a normative study (Losey et al. 1998) and comparable to the one used in other centers (Regan et al. 1992; Barton et al. 1995).

Follow-up evaluations 11 months after the lesion confirmed normal visual motion perception, while her severe FfM perception deficit persisted (same tests as above). FfM processing was further evaluated and confirmed in the present study using a slightly modified design to be used during the electroencephalography (EEG) experiments (see next section). Written informed consent was obtained and the experiments were approved by the local Ethical Committee of the University Hospital of Geneva in accordance with the Declaration of Helsinki.

Stimuli

Stimuli used were identical to those described previously (Blanke et al. 2007) and presented on a 20-inch computer monitor (Sony Trinitron Multiscan model no. GDM-20SE1VT; frame rate, 70 Hz; 640 pixels × 480 pixels), with a viewing distance of 100 cm. Stimuli consisted of white dots (32.5 cd/m^3 as mean luminance) randomly positioned on a black background. Each stimulus contained 1000 dots (each dot had a diameter of 0.068°), randomly positioned to maintain constant density over the presentation field. Dots were programmed to be displaced with a velocity of 2°/s during the presentation. Random dot kinematogram stimuli were presented for 300 ms and alternated with a white fixation cross displayed on a black background, presented for 1500 ms. This was used to facilitate fixation during the task as the patient was asked to maintain the gaze fixed during stimulus presentation.

A borderless static area representing a capital letter "*E*" was defined in the center of the presentation field (12° × 12°) and covered 28.6 % of the presentation area. This letter could be oriented to the right (canonical) or left. Dots outside this area were plotted at random locations (for a random life time between 15 and 300 ms) giving the impression of flickering dots. Inside the area, dots could be either noise dots, equivalent to those located outside the form, or signal dots moving coherently. The proportion of dots moving coherently inside the form defined the percentage of coherent motion (% CM). Dots moving out of the form area reappeared on the opposite side such that the density was held constant. The motion direction and the form orientation of each FFM stimuli in each block varied independently and randomly between left and right. Stimuli were produced beforehand using the Cogent Graphics Matlab toolbox (http://www.vislab.ucl.ac.uk/cogent.php) and displayed during the experiment using E-prime (Psychology Software Inc., Pittsburgh, PA, USA).

Task

Two tasks with physically identical stimuli were performed by the patient during the EEG experiment. In the form-from-motion task (FfM task), the patient was asked to indicate the orientation of the letter "*E*" (whether the arms of the letter were directed toward the left or right). In the visual motion task (VM task), the patient had to indicate the direction of the dots moving coherently (left or right). Therefore, depending on the task, the patient had to either focus on the orientation of the depicted letter (FfM task), or on the direction of the coherent motion within the letter (VM task) to be able to respond correctly (left or right button press; the responses were collected via E-prime response box, Psychology Software Inc., Pittsburgh, PA, USA).

Data recording and analysis

Control participants

The normative data used to initially test the present patient were obtained from a group of healthy participants ($n = 34$; age range from 21 to 69), reported in a normative study (Losey et al. 1998). To further describe the patient's deficit, comparisons were made against a group of brain-damaged patients ($n = 8$; 54.1 ± 16.9; mean age ± standard deviation), reported in a previous publication (Blanke et al. 2007), and a group of healthy subjects of similar age ($n = 11$; 56.4 ± 9.0; mean age ± SD).

Patient behavior

To confirm the patient's FfM perception deficit, we performed two preparatory measurements before the EEG was recorded. On both occasions, her psychophysical FfM and VM thresholds were determined. This was done 8 days before the EEG recording as well as on the day of the EEG recording to ensure the stability of her FfM and VM thresholds (12 months after lesion onset).

Based on her FfM performance, we selected three different levels of % CM for the EEG experiment that reflected three different levels of FfM perception: 0 % CM (FfM perception absent in the patient and healthy subjects), 20 % CM (successful FfM perception in healthy subjects, but chance performance in the patient) and 100 % CM (successful FfM perception in the patient and healthy subjects). In addition, the patient's VM perception was also tested for the same % CM levels, for which she performed normally at all three levels. For the patient's performance, see Fig. 1c.

EEG acquisition and pre-processing

Continuous EEG was acquired in a Faraday cage, with a Geodesics Netamps system (Electrical Geodesics Inc., Eugene, OR, USA) from 128 electrodes (impedances <50 kΩ; vertex reference; 500 Hz sampling rate: band pass filter 0.1–200 Hz). EEG epochs were calculated from 100 ms before to 400 ms after stimulus onset, band pass filtered between 1 and 40 Hz and averaged separately for each condition (0, 20 and 100 % CM) to calculate the event-related potential (ERP). In addition to the application of an automated artifact criterion of ±100 μV, data were visually inspected to reject epochs with transient noise like eyeblinks, eye movements and muscular artifacts. Electrodes located laterally and above the eyes were used to detect eye movements as the patient was told not to explore the stimulus, but to maintain the gaze fixed. The baseline was defined as the mean value of the averaged amplitude from 100 ms before to 0 ms (stimulus onset). Signal from electrodes with artifacts was replaced with interpolated data from neighboring electrodes. ERP data were down-sampled to a 111-channel montage used in the estimation of the inverse solution. All pre-processing steps (filtering, baseline correction and interpolation) were also applied to single events without artifacts and used to calculate the ERPs. These single events were later used for statistical analysis.

ERP mapping

ERPs from 0 to 400 ms were analyzed using a spatio-temporal clustering algorithm. The rationale behind this approach relies on the fact that ERP maps do not change randomly over time, but remain stable for a period of time before changing to another stable configuration (this dynamics reflects the succession of macroscopic brain processing steps). Moreover, since a given spatial configuration of the electric field on the scalp corresponds to a specific contribution and/or distribution of underlying neuronal generators, different topographical map configurations between experimental conditions reflect distinct brain activation patterns (Lehmann et al. 1987; Michel et al. 1999, 2001; Murray et al. 2008; Pascual-Marqui et al. 1995; Brunet et al. 2011). This method was applied to the dataset from each task to reveal the distinct dynamics of brain activity in each experimental condition, showing when their corresponding ERP maps differed.

To identify the most dominant scalp topographies appearing in the ERPs over time, the algorithm used was based on a modified *k* means approach, with the optimal number of dominant topographical maps being determined by a cross-validation criterion (see Brunet et al. 2011; Murray et al. 2008, for details). Next, the condition specificity of the dominant scalp topographies was tested statistically. To do so, ERP maps were fitted back to the single trials by computing their frequency of occurrence and global explain variance (GEV; corresponding to the goodness of fit of a map during a given time period). These dependent variables were then subjected to statistical analysis using unpaired *t* tests with single trials as repeated measures. A similar analysis procedure has previously been applied to study a wide variety of cognitive processes in healthy subjects [such as perception (Lopez et al. 2011), attention (Plomp et al. 2009), social interaction (Thirioux et al. 2010, 2014)] as well as in clinical populations (Michel and Murray 2012).

Distributed source localization

Electrical brain sources underlying the ERP maps of interest (i.e., those which differ between conditions) were estimated using the local autoregressive average method [LAURA, (Gonzalez Andino et al. 2001; Grave de Peralta Menendez et al. 2004)]. Importantly, the brain lesion was taken into account in the spherical model with anatomical constraints implemented for the inverse solution (Spinelli et al. 2000). That is, the patient's structural MRI was used to compute the lead field and to position the solution points in individual gray matter (around 4900 points evenly distributed). Finally, inverse solution results were projected onto the brain template from the Montreal Neurological Institute (MNI).

The analysis was performed using the Cartool software by Denis Brunet (http://brainmapping.unige.ch/cartool).

Results

Behavior

The patient's deficit in FfM perception (elevated perceptual threshold of 20 % CM) and normal VM perception (perceptual threshold at 0.95 % CM) was initially defined on the basis of normative data (Losey et al. 1998). For the purposes of the present study, additional comparisons were conducted: first, with a group of brain-damaged control patients (perceptual thresholds at 8.7 % CM ± 4.4 SD for FfM and at 0.8 % CM ± 0.4 SD for VM); secondly, with a group of age-matched healthy individuals (perceptual threshold at 9.8 % CM ± 5.5 SD for FfM and at 0.8 % CM ± 0.39 SD for VM). The patient's performance was evaluated with respect to the controls, using corresponding subsequent *t* distributions from which the 99 % confidence prediction intervals were derived and perception deficit inferred (Blanke et al. 2007). Two tests conducted 1 week apart, before the EEG

recording, confirmed the stability of pathological FfM perception (with the patient's perceptual thresholds at 19.0 and 20.9 %), while VM perception remained normal (1.2 and 0.7 %).

During the EEG experiment, the patient's performance was consistent with her previously defined deficit (Fig. 1c). As expected, when there was no directed/coherent motion presented (i.e., 0 % CM stimuli), the patient was at chance level in both tasks (FfM task: 52.8 % ± 5.8 SD; VM task: 52.5 % ± 3.1 SD). Critically, for the 20 % CM stimuli, the patient was at chance level in the FfM task (48.8 % ± 6.2 SD of correct responses), while in the VM task, she was able to perceive the coherent motion direction from the same FfM stimuli (90.6 % ± 6.0 SD correct). Finally, for the 100 % CM stimuli, her performance was high in both tasks (FfM task: 98.0 % ± 1.0 SD; VM task: 98.4 % ± 1.0 SD). In summary, the behavioral results during the EEG recoding were consistent with the evaluation carried out prior to the EEG study: in the VM task which is associated with dorsal motion processing, the patient did not show any impairment whereas in the FfM task, additionally associated with ventral processing, persistent perceptual deficits were found.

ERP mapping

ERPs obtained for each condition were subjected to a topographical cluster analysis (see "Materials and methods"). This method entails segmenting the temporal course of activity into distinct dominant scalp map configurations. Identified ERP maps were then subjected to statistical analysis at the single trial level (*t* test) to demonstrate their specificity with regard to the different conditions.

FfM task

As depicted in Fig. 2, the temporal cluster analysis, applied to ERPs from the three conditions, identified a total of ten maps during the period from stimulus onset to 400 ms. Importantly, of the ten ERP maps, six differentiated the experimental conditions over three consecutive time periods: 160–180 ms (maps 4 and 5), 180–270 ms (maps 6 and 7) and 270–310 ms (maps 8 and 9). The topographic differences between conditions were further confirmed by statistical analysis applied on both the frequency of occurrence of the maps and their GEV (see Table 1 and "Data recording and analysis" for details of the statistics). During the first period (160–180 ms), experimental conditions that included coherent motion FfM stimuli (20 and 100 % CM) showed the same ERP map, 5, whereas a different ERP map, 4, was found in the 0 % CM condition. During the two following time periods (180–270 and 270–310 ms), the 100 % CM condition (successful FfM perception) was characterized by two ERP maps (ERP maps 7 and 9), while the 0 and 20 % CM conditions (FfM perception absent/failed) were characterized by distinct ERP maps (maps 6 and 8). Importantly, the temporal dynamics of the maps differentiating the conditions in the present patient echoed the results obtained in healthy subjects reported in an earlier study by Schoenfeld et al. (2003), where three time periods (195–230, 230–340 and 340–470 ms) were linked to different functional processing steps in FfM perception.

In summary, the analysis of ERP topographies showed that each experimental condition evoked a specific sequence of three topographical maps during the time period from 160 to 310 ms (see Fig. 2 for illustration). During the first period (160–180 ms), conditions containing coherent motion (20 and 100 % CM) were distinguished from the condition without coherent motion (0 % CM). This was independent of FfM perception and linked to motion processing. The second and third periods (180–270 and 270–310 ms) differentiated absent/failed (0 and 20 % CM) from successful FfM perception (100 % CM). Note that before 160 ms and after 310 ms, the three conditions presented identical ERP maps (respectively, maps 1, 2, 3 and map 10), with no statistical differences found at any other time periods and for any other ERP maps.

VM task

The same analysis of ERP topographies was applied to the control VM task. As illustrated in Fig. 3, a total of nine ERP maps were identified, including four ERP maps that differed between the conditions. These topographical differences were found during two consecutive time periods, 150–170 ms (ERP maps C and D) and 170–190 ms (ERP maps E and F) and were confirmed by statistical analysis (duration; GEV, see Table 2). Conditions with coherent motion (20 and 100 % CM) were characterized during both time periods by the same maps (ERP maps D and F), while the 0 % CM condition was characterized by two other maps (ERP maps C and E). To summarize, topographical analysis of ERP revealed that from 150 to 190 ms, absent VM perception (0 % CM condition) evoked a different sequence of topographical maps than conditions associated with successful VM perception (20 and 100 % CM conditions).

Source localization

FfM task

After having identified the ERP maps that were specific to the different conditions, we applied the source

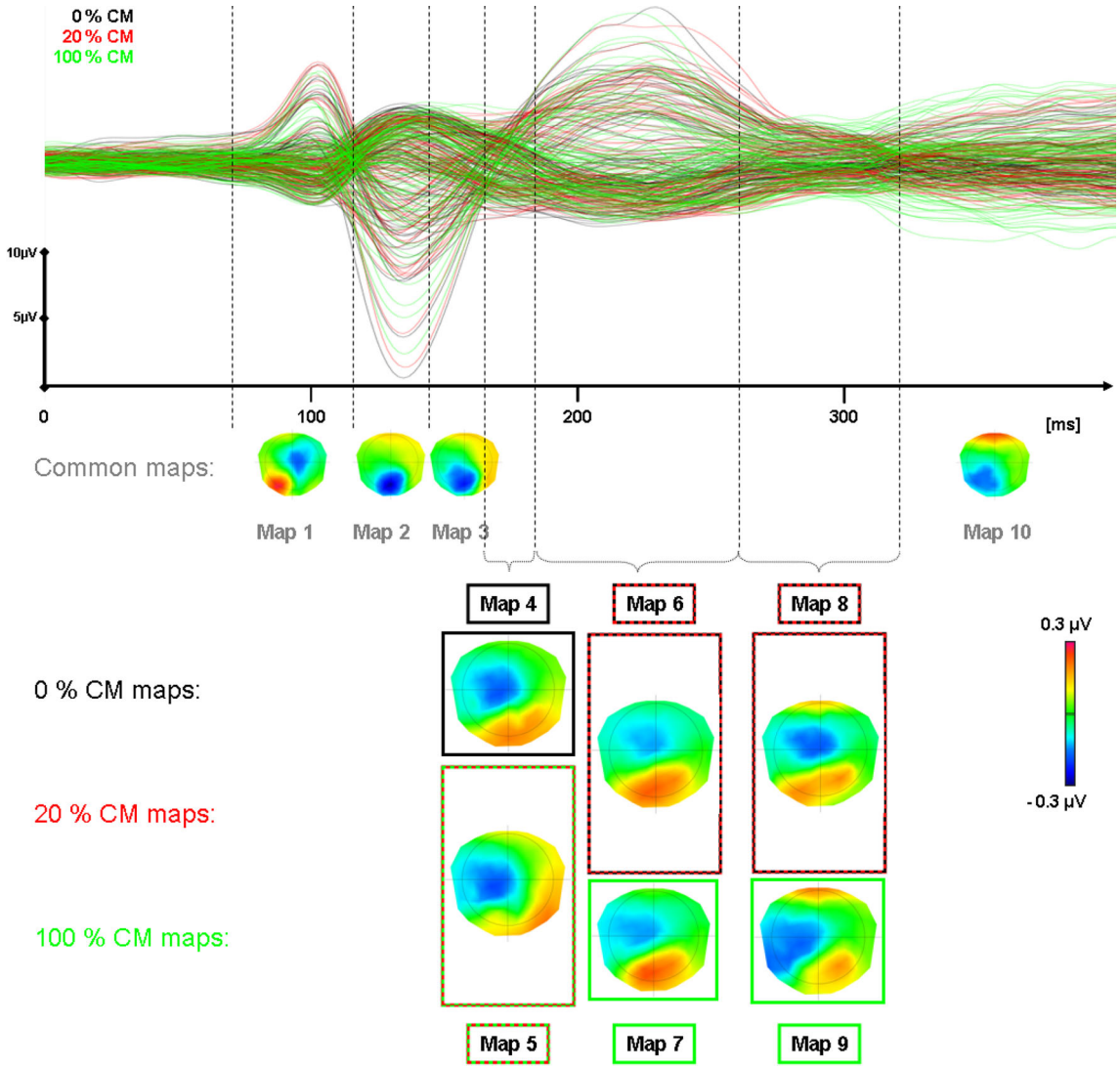

Fig. 2 ERP-topographical analysis: FfM task. In the *upper half of the figure*, superimposed ERP traces of all recorded scalp electrodes are shown for the 0 % (*black*), 20 % (*red*) and 100 % CM (*green*) conditions from stimulus onset to 400 ms. In the *lower half of the figure*, results from the topographical clustering analysis are shown by depicting the ERP maps found in the different experimental conditions. Successful FfM perception was associated with ERP maps 7 and 9 in the time period from 180 to 310 ms, whereas ERP maps 6 and 8 in the same time period were associated with absent FfM perception. The presence of coherent motion (20 and 100 % CM) is characterized by the presence of map 5 from 160 to 180 ms; consequently, each condition presents a specific sequence of three ERP maps during the 160–310 ms time period

reconstruction model built using the patient's brain with its anatomical characteristics due to the lesion (see detailed descriptions in "ERP mapping"; and results summary in Table 3A). As illustrated in Fig. 4, successful FfM perception (indexed by ERP maps 7 and 9) was characterized by brain activations in extra striate cortex including both dorsal and ventral regions, with first stronger activity in parieto-occipital cortex and weaker activations in temporo-occipital regions (ERP map 7, 180–270 ms), followed by additional activity in the left posterior temporal cortex and bilateral frontal regions (ERP map 9, 270–310 ms). In contrast, absent/failed FfM perception elicited much weaker activity at first (map 6; 180–270 ms), followed by activity limited to the temporo-occipital cortex (map 8; 270–310 ms). This strongly focused posterior activation observed for absent/failed FfM perception contrasted with the distributed set of more dorsal and frontal regions activated during successful FfM perception. Based on previous studies (Wang et al. 1999; Schoenfeld et al. 2003), brain activations were expected initially in dorsal regions (e.g., posterior temporal) followed by a shift of activity to ventral regions (e.g., temporo-occipital cortex). Compared to the patterns from neurotypical subjects, activations in the present patient showed two main differences: stronger

Table 1 Fitting for the FfM task: ERP map comparison for each time period and each condition (% CM)

Time period	160–180 ms	180–270 ms	270–310 ms
CM			
Maps comparison	4 vs. 5	6 vs. 7	8 vs. 9
0 %			
GEV	$t_{216} = 4.21$	$t_{216} = 12.20$	$t_{216} = 7.29$
	$p < 0.0001$	$p < 0.0001$	$p < 0.0001$
Occurrence frequency	$t_{216} = 2.11$	$t_{216} = 2.770$	$t_{216} = 2.86$
	$p < 0.05$	$p < 0.01$	$p < 0.01$
20 %			
GEV	$t_{229} = 1.53$	$t_{229} = 11.01$	$t_{229} = 7.50$
	$p = 0.13$	$p < 0.0001$	$p < 0.0001$
Occurrence frequency	$t_{229} = 2.49$	$t_{229} = 2.67$	$t_{229} = 2.24$
	$p < 0.5$	$p < 0.01$	$p < 0.05$
100 %			
GEV	$t_{178} = 7.22$	$t_{178} = 3.80$	$t_{178} = 0.76$
	$p < 0.0001$	$p < 0.0005$	$p = 0.45$
Occurrence frequency	$t_{178} = 3.46$	$t_{178} = 3.39$	$t_{178} = 3.40$
	$p < 0.001$	$p < 0.001$	$p < 0.01$

Statistical results are shown for the GEV and frequency of occurrence of each ERP map

activity in the parieto-occipital cortex followed by co-activation of the dorsal and ventral regions (Fig. 4).

VM task

EEG source reconstruction was also applied on the topographical maps that dissociated the conditions in the VM task. The results, summarized in Table 3B (see also Fig. 5), revealed stronger activations along the dorsal stream for successful VM perception during the two time periods of interest (ERP maps D and F, respectively, occurring between 150–170 and 170–190 ms) as compared to absent VM perception (characterized by ERP maps C and E).

Discussion

In this study, we investigated FfM perception in a patient suffering from a selective perceptual deficit for FfM following focal right medial occipital brain damage. Despite her abnormal perceptive threshold in FfM perception, the patient was able to perceive FfM stimuli at high signal to noise ratio (100 % CM), allowing us to investigate evoked brain activity related to successful and absent/failed FfM perception. In the critical 20 % CM condition, the patient was not able to perceive FfM, but perceived VM normally. Analysis of the dynamics of ERP topographies revealed three distinct stages of FfM processing: first, an early processing step (160–180 ms) linked to motion processing, followed by two distinct time periods from 180 to 270 and from 270 to 310 ms, which distinguished successful FfM perception from absent/failed FfM perception. Successful FfM perception was characterized during the second time period by strong activations in parieto-occipital regions (rostral part of the dorsal stream). During the third period, this activity was supplemented by co-activation of the posterior temporal (lateral part of the dorsal stream) and the temporo-occipital regions (ventral stream). The temporal dynamics of the three processing steps for the present patient were similar to that reported in healthy subjects, albeit the underlying patterns of brain activation were different, suggesting the existence of multiple brain circuits involved in FfM perception.

FfM perception

Anatomical perspective

Similar to the present case, a number of studies have reported a specific FfM perceptual deficit following ventral brain lesions (Blanke et al. 2007; Vaina 1989; Regan et al. 1992). Also, in some of the patients, the brain damage led to an abnormal increase of FfM perceptual threshold, but not to complete FfM blindness. Interestingly, other cases of brain lesions have been described where the same FfM deficit was linked to damage in dorsal regions, either including the more lateral part or the more parietal part (Blanke et al. 2007; Regan et al. 1992; Cowey and Vaina 2000; Schenk and Zihl 1997; Vaina et al. 2010). Globally, these studies have causally demonstrated the role of both ventral and dorsal regions in FfM perception.

The involvement of both neuronal visual pathways in FfM processing has been confirmed by imaging studies showing FfM-related activation of the dorsal area MT+/V5, as well as ventral and lateral occipital regions such as the latero-occipital cortex (LOC) and ventro-occipo-temporal cortex (Wang et al. 1999; Gulyas et al. 1994; Schoenfeld et al. 2003). In the present case study, electrical brain imaging analysis revealed that successful FfM perception (at 100 % CM) was also associated with multiple activations in both the dorsal and ventral regions. The dorsal activity observed in the posterior temporal regions likely corresponds to area MT+/V5. The implication of MT+/V5 was expected because of its well-known central role in visual motion processing (Born and Bradley 2005), as exemplified in monkey electrophysiological recordings investigating the neural correlates of moving surfaces (Andersen and Bradley 1998; Bradley et al. 1998; Dodd et al. 2001; Grunewald et al. 2002), or in human imaging studies of FfM and Structure from Motion perception (SfM is a 3D version of FfM supported by different brain

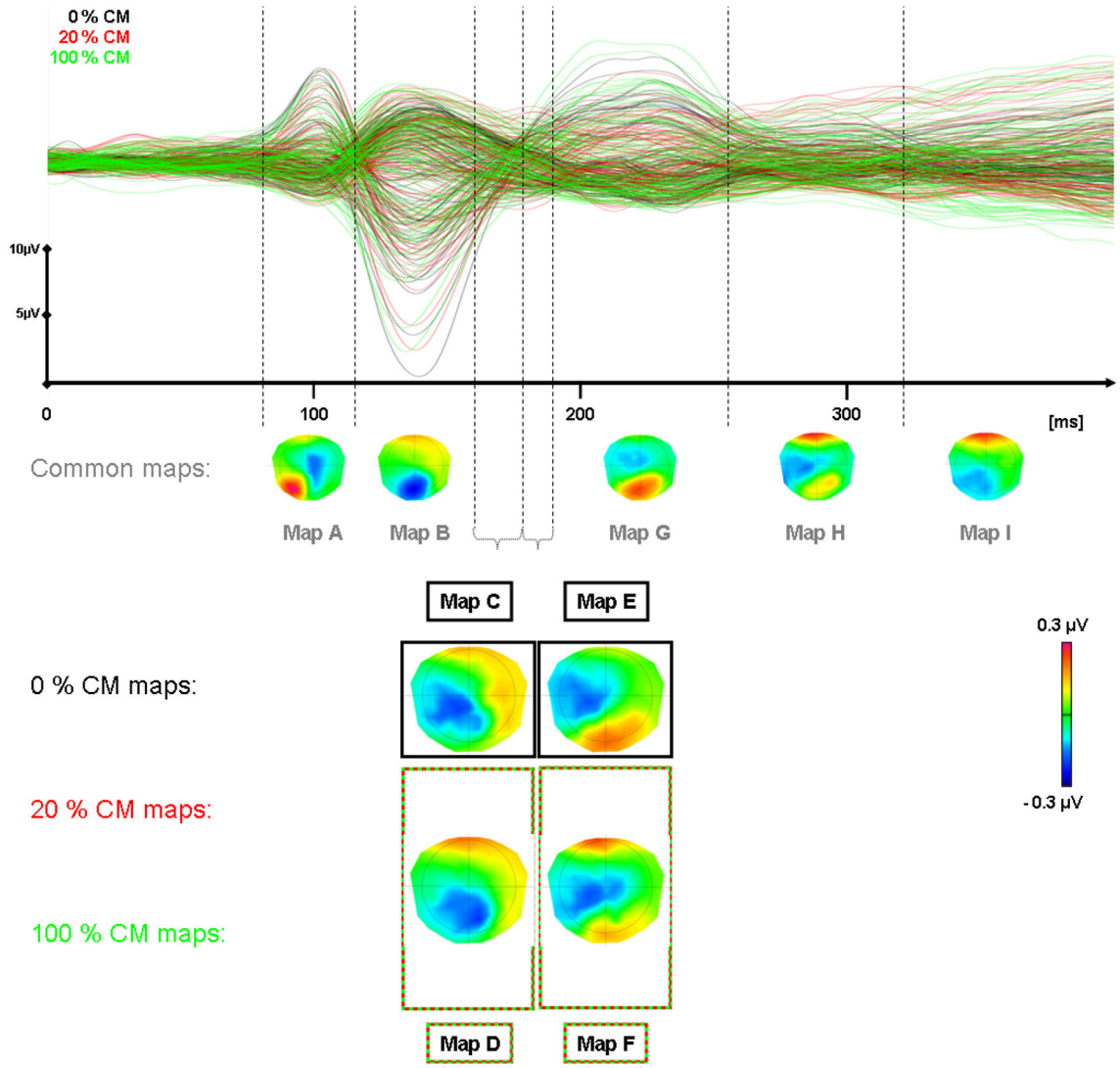

Fig. 3 ERP-topographical analysis: VM task. In the *upper half of the figure*, superimposed ERP traces of all recorded scalp electrodes are shown for the 0 % (*black*), 20 % (*red*) and 100 % CM (*green*) conditions from stimulus onset to 400 ms. In the *lower half of the figure*, results from the topographical clustering analysis are shown by depicting the ERP maps found in the different experimental conditions. Successful VM perception (20 and 100 % CM) was associated with ERP maps D and F in the time period from 160 to 190 ms, whereas ERP maps C and E in the same time period were associated with absent VM perception (0 % CM)

circuits; for a review see (Born and Bradley 2005) and further discussion below). Another lateral posterior region located more ventrally was found to be activated, presumably the LOC mainly known for being implicated in static object perception (Grill-Spector et al. 1998; Malach et al. 1995). Moreover, its role in form processing appears to be independent of the visual cue; LOC activity can relate to perceptual persistence of motion-defined grouping (Ferber et al. 2003), or can be adapted to a given shape regardless of the cue used (Self and Zeki 2005). Furthermore, the strongest activations measured for successful FfM perception and not observed for absent/failed FfM perception, were located in the parieto-occipital regions, part of the dorsal pathway, possibly corresponding to areas V3A and/or IPS. While parieto-occipital activity in response to FfM processing has not been reported in brain imaging studies (Schoenfeld et al. 2003; Wang et al. 1999; Gulyas et al. 1994), these supplementary visual motion areas were found to be fundamental for 3D motion and more specifically for SfM processing (Vanduffel et al. 2002; Orban et al. 1999; Paradis et al. 2000; Peuskens et al. 2004; Gulyas et al. 1994; Andersen 1989; Zhuang et al. 2008; Brouwer and van Ee 2007; Cottereau et al. 2014). Interestingly, overlapping activations for SfM and line drawings have been reported in an area located in the vicinity of the IPS region (Murray et al. 2003), which suggests its potential role in processing related to form perception. From a purely anatomical perspective, brain

activity evoked by successful FfM perception in the present patient echoed the converging evidence from both lesion case studies and brain imaging studies, pointing to the role of both the dorsal and the ventral streams in FfM processing. However, the observation of activations in the parieto-occipital regions is noteworthy: while being novel compared to brain imaging studies, it corroborates the cases of FfM perceptual deficit after parieto-occipital lesions.

Table 2 Fitting for the VM task: ERP map comparison for each time period and each percentage coherent motion (% CM)

Time period	150–170 ms	170–190 ms
CM		
Maps comparison	C vs. D	E vs. F
0 %		
GEV	$t_{170} = 5.89$	$t_{170} = 6.02$
	$p < 0.0001$	$p < 0.0001$
Occurrence frequency	$t_{170} = 1.98$	$t_{170} = 1.10$
	$p < 0.5$	$p = 0.27$
20 %		
GEV	$t_{188} = 7.09$	$t_{188} = 2.45$
	$p = 0.0001$	$p < 0.05$
Occurrence frequency	$t_{188} = 4.23$	$t_{188} = 2.31$
	$p < 0.0001$	$p < 0.05$
100 %		
GEV	$t_{197} = 6.62$	$t_{197} = 1.56$
	$p < 0.0001$	$p = 0.12$
Occurrence frequency	$t_{197} = 4.84$	$t_{197} = 2.22$
	$p < 0.0001$	$p < 0.05$

Statistical results are shown for the GEV and frequency of occurrence of each ERP map

Temporal dynamics

The ERP mapping analysis revealed similar dynamics of scalp topographies in the present patient compared to healthy subjects from a comparable study (Schoenfeld et al. 2003). That is, in the FfM task, experimental conditions were differentiated by three processing steps: a first period (160–180 ms) linked to motion processing (see "VM control task" for detailed discussion), and second and third periods (180–270 and 270–310 ms) linked to FfM processing. Regarding the brain sources underlying this sequence of stable processing states, the first period was equivalent to normal subjects, with activation in dorsal regions. However, while only ventral regions were activated in normal subjects during the second and third processing steps, we found activity, respectively, in parietal regions followed by co-activation of dorsal and ventral regions. Importantly, we did not observe these specific patterns in the absent/failed FfM perception condition. Analogous co-activation of dorsal and ventral regions involving parieto-occipital regions has been reported in a study investigating SfM processing (Jiang et al. 2008). In that study, the timing overlap (206–355 ms) between

Table 3 Major brain activations (strongest to weakest) differentiating conditions

(A) FfM task[a]			
Time period	160–180 ms	180–270 ms	270–310 ms
0 % CM	Left parieto-occipital	Right parieto-occipital	Left temporo-occipital
	Left posterior temporal	Left parieto-occipital	Right parieto-occipital
20 % CM	Left parieto-occipital	Bilateral temporo-occipital	Right temporo-occipital
100 % CM	Left posterior temporal	Left parieto-occipital	Left parieto-occipital
	Right temporo-occipital	Right parieto-occipital	Left posterior temporal
	Left temporo-occipital	Left temporo-occipital	Bilateral frontal
			Right parieto-occipital
			Left temporo-occipital

(B) VM task[b]		
Time period	150–170 ms	170–190 ms
0 % CM	Right parieto-occipital	Left temporo-occipital
	Left temporo-occipital	Right parieto-occipital
	Left parieto-occipital	Right temporo-occipital
20 % CM	Left posterior temporal	Left parieto-occipital
100 % CM	Right parieto-occipital	Bilateral frontal
	Right posterior temporal	Right parieto-occipital
		Left posterior temporal

[a] Three time periods between 160 and 310 ms. [b] Two time periods between 160 and 190 ms

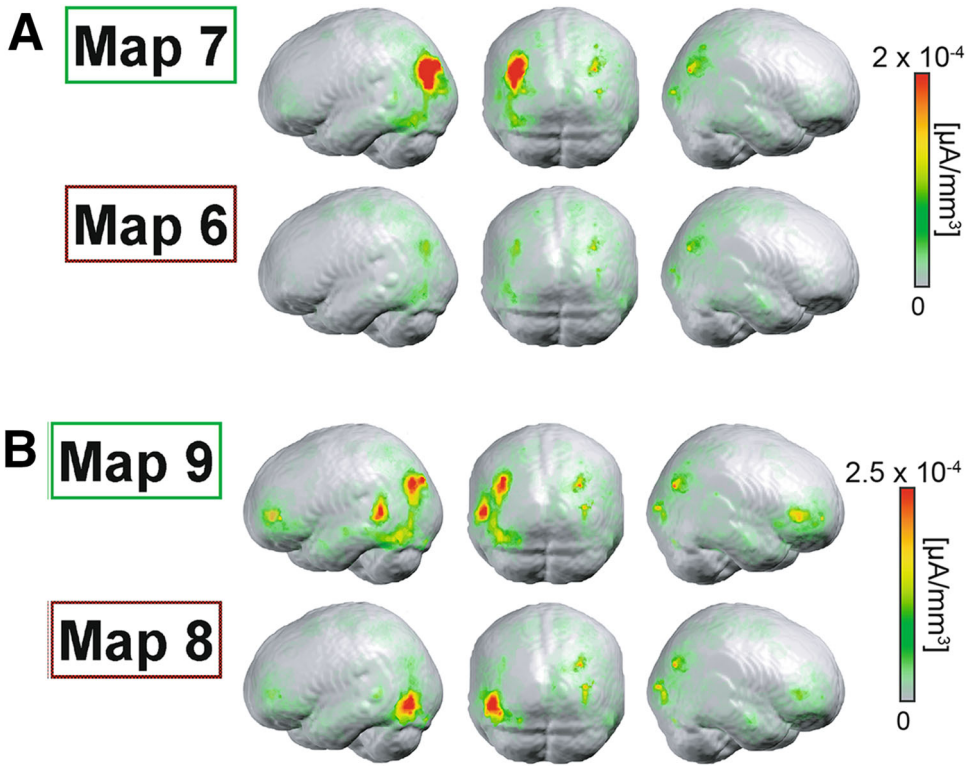

Fig. 4 Inverse solution: brain activation related to FfM processing. **a** Brain activity corresponding to maps 7 and 6 occurring between 180 and 270 ms are shown for successful FfM perception and for absent FfM perception, respectively. Brain activations related to successful FfM perception (map 7) were located in dorsal regions: left parieto-occipital cortex (maximum), right parieto-occipital cortex (with weaker activations in posterior temporal cortex and left temporo-occipital cortex). **b** Brain activity corresponding to maps 9 and 8 occurring between 270 and 310 ms are shown for successful FfM perception and for absent FfM perception, respectively. Brain activations related to successful FfM perception (map 9) were located in dorsal regions [left parieto-occipital cortex (maximum), left posterior temporal cortex, right parieto-occipital cortex] and in ventral regions (left temporo-occipital cortex and in bilateral frontal regions)

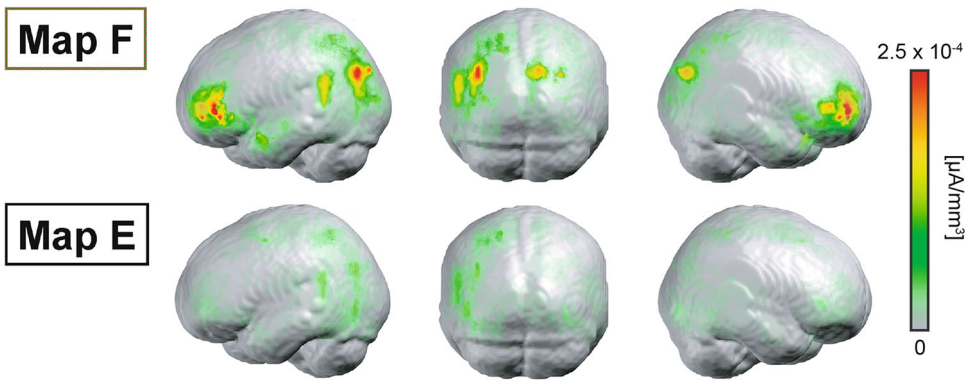

Fig. 5 Inverse solution: brain activation related to VM processing. Brain activity corresponding to maps F and E occurring between 170 and 190 ms are shown for successful VM perception and for absent VM perception, respectively. Brain activity related to successful VM perception (map F) was located in the bilateral frontal cortex and in the dorsal regions (bilateral parieto-occipital cortex and left posterior temporal cortex)

parieto-occipital, early posterior temporal and later temporo-occipital activations was the same as in the third processing step found in the present patient. In summary, analysis of the temporal dynamics revealed that while the three processing steps linked to FfM perception described in normal subjects were preserved in the patient, successful FfM perception was associated with activations of the parieto-occipital regions and co-activation of dorsal and

ventral regions. This pattern of brain activations has not been observed in FfM studies in healthy subjects, but was previously described in studies investigating SfM processing.

FfM perception and the model of the visual system

While it is clear that the posterior temporal region of the dorsal stream and temporo-occipital regions of the ventral stream are essential for FfM processing, the role of the parieto-occipital regions remains unclear. On the one hand, studies of brain-lesioned patients revealed some cases of FfM deficit following parieto-occipital damage, providing a causal link between the most rostral regions of the dorsal pathway and FfM perception. On the other hand, brain imaging studies of FfM perception have not reported any activity in these parieto-occipital regions. That same brain region has been functionally linked to SfM processing in both brain lesion studies (Cowey and Vaina 2000; Vaina 1989) and imaging studies (Jiang et al. 2008; Zhuang et al. 2008), and while FfM and SfM have been functionally double dissociated in brain lesion studies (Vaina 1989; Vaina and Gross 2004), it could be the case that FfM and SfM are partly supported by some common circuits within the dorsal pathway before being segregated.

This hypothesis is reinforced by further refinements of the classic visual system model that suggest the existence of different circuits within the dorsal pathway [see (Matheson and McMullen 2010) for a human model and (Galletti and Fattori 2003) for a similar model in monkey]. For instance, comparison of brain responses to different types of motion based on complexity (e.g., random motion, coherent motion, FfM and SfM) revealed a gradient of functional specificity among the dorsal regions from the more lateral parts to the most rostral parts, while no functional specificity was observed in the regions of the ventral pathway (Paradis et al. 2000; Orban et al. 1999). Similarly, patient studies seem to suggest that brain damage to temporal regions is more often linked to FfM perceptual deficits, whereas lesions extending toward the parietal lobe are linked to both SfM and FfM perceptual deficits (Schenk and Zihl 1997; Vaina 1989; Cowey and Vaina 2000). Accordingly, some authors (Vaina et al. 2010; Matheson and McMullen 2010; Castelo-Branco et al. 2006) have suggested that FfM processing could be shared between two dorsal sub-streams: a lateral and a rostral occipito-parietal pathway (whereas SfM processing can dissociate them since it involves solely the rostral part). Also, placing FfM processing at functional cross-roads within the dorsal pathway implies that the dedicated brain circuits are more likely to be versatile. This view explains the location diversity in brain-damaged patients leading to FfM perceptual deficits (Blanke et al. 2007; Vaina et al. 2010; Matheson and McMullen 2010; Schenk and Zihl 1997; Cowey and Vaina 2000; Regan et al. 1992), as well as cases of functional dissociation between FfM and SfM in lesioned patients (Vaina 1989; Vaina and Gross 2004). Moreover, in the case of the present patient, the versatility of the brain circuits involved in FfM processing could explain the activation of the rostral part of the dorsal stream in successful FfM perception. This contribution may however be too small to be measured in normal subjects using neuroimaging approaches, but could be revealed in the present patient due to the impact of the ventral lesion on normal FfM processing. Furthermore, here the involvement of these parieto-occipital regions was followed by dorsal and ventral co-activations, as reported in purely SfM processing (Jiang et al. 2008), thus demonstrating the importance of the interplay between the dorsal and ventral regions involved in this brain circuit. In comparison, when the percentage of coherent motion was too low for the patient (but large enough for normal subjects) to perceive FfM, motion information was processed by the more lateral part of the dorsal stream but could not be subsequently integrated into a form; the most dorsal circuits were not activated and neither parieto-occipital activity nor dorsal and ventral co-activation was found.

VM control task

Temporal clustering of the ERP maps revealed different topographies between 150 and 190 ms for incoherent (0 % CM) and coherent motion (20 and 100 % CM). The latency of these differences is consistent with previous studies showing that processing of coherent motion occurs around 170 ms (Heinrich 2007; Kuba et al. 2007; Niedeggen and Wist 1999; Mercier et al. 2009). During this time window, stronger activations were found for the coherent motion conditions in the posterior temporal, parieto-occipital and parietal regions (see Fig. 5). As discussed previously, the posterior temporal cortex activation most likely corresponds to the area MT+/V5 activity (de Jong et al. 1994; Dupont et al. 1994, 1997; Goebel et al. 1998; Tootell et al. 1995; Tootell and Taylor 1995; Watson et al. 1993) and activations in the parieto-occipital cortex may correspond to area V3a and/or IPS (Braddick et al. 2000; Sunaert et al. 1999). Moreover, the parietal activity matched the activation of area V6 (Fattori et al. 2009; Pitzalis et al. 2006, 2010), known to be involved in motion processing and self-motion recognition (Pitzalis et al. 2010, 2013). These results show distributed activations over the dorsal pathway for successful motion perception, with a similar dynamic as reported in normal subjects. Also, it is interesting to note that, as in the FfM task, brain activations related to the VM task were mainly localized in the contralesional hemisphere.

Study limitations

Like any single case study, the present report has to be considered with caution and it would benefit from extension to a larger cohort. Nevertheless, patients presenting a specific perceptual deficit are rare, and comparison between patients is rendered difficult due to their dissimilarity (e.g., lesion size, location and diversity of deficits). Another limitation of this case study concerns the comparison of brain activation with precisely age-matched controls performing exactly the same task. However, the results showed three processing steps with timings that are equivalent to what has been reported in the literature. Although some brain activity patterns are different from what have been previously described, this study provides insights to bridge the gap between lesion studies and imaging studies in healthy participants. More generally, the present findings are coherent with several previous studies that have reported alternative functional circuits in brain-damaged patients, potentially due to lateral and/or feedback connections (see for instance the case of patients with intact MT+/V5, suffering from motion deficit due to damage in the ventral region (Gilaie-Dotan et al. 2013), for other cases and additional discussion see (Vaina et al. 2000, 2010; Gilaie-Dotan 2015). Hence, the use of brain imaging methods in brain-damaged patients may provide important insights toward a better understanding of the role of auxiliary pathways in visual deficits and can thus refine the current model of the visual system.

Conclusion

In the present case report, we applied ERP topographical analysis and brain source localization to investigate an FfM perceptual deficit following medial occipital brain damage. Our results extend previous findings where successful FfM perception was shown to activate both dorsal and ventral visual streams during three distinct time windows. While the earliest time period is dedicated to elementary motion processing and involves the dorsal stream, the two later periods are linked to FfM processing. In comparison to normal subjects, during these later periods, strong involvement of the parieto-occipital regions preceding co-activation of the dorsal and ventral regions was revealed. Though the timings of the three processing steps were preserved, this atypical pattern of brain activation (only observed for successful FfM perception) can be explained by the implication of the more rostral part of the dorsal pathway, due to the location of the brain lesion. These results suggest the existence of an auxiliary brain circuit of dorso-ventral interactions involved during successful FfM processing.

Acknowledgments The authors would like to express their gratitude to the patient for her time and her patience during the investigations. We also would like to thank Arnaud Saj for providing precious information regarding patient history and we are extremely grateful to Nihaad Paraouty, Grace Edwards and Douglas McLelland for English editing. This research was funded by the Swiss National Science Foundation (Grants 310000-114008 and 3200B0-104100) and the Swiss Center for Affective Sciences. The Cartool software (http://brainmapping.unige.ch/cartool) has been programmed by Denis Brunet, from the Functional Brain Mapping Laboratory, Geneva, Switzerland, and is supported by the Center for Biomedical Imaging (CIBM) of Geneva and Lausanne. This experiment was realized using Cogent Graphics developed by John Romaya at the LON at the Wellcome Department of Imaging Neuroscience.

References

Andersen RA (1989) Visual and eye movement functions of the posterior parietal cortex. Annu Rev Neurosci 12:377–403. doi:10.1146/annurev.ne.12.030189.002113

Andersen RA, Bradley DC (1998) Perception of three-dimensional structure from motion. Trends Cogn Sci 2(6):222–228

Barton JJ, Sharpe JA, Raymond JE (1995) Retinotopic and directional defects in motion discrimination in humans with cerebral lesions. Ann Neurol 37(5):665–675. doi:10.1002/ana.410370517

Blanke O, Brooks A, Mercier M, Spinelli L, Adriani M, Lavanchy L, Safran AB, Landis T (2007) Distinct mechanisms of form-from-motion perception in human extrastriate cortex. Neuropsychologia 45(4):644–653

Born RT, Bradley DC (2005) Structure and function of visual area MT. Annu Rev Neurosci 28:157–189. doi:10.1146/annurev.neuro.26.041002.131052

Braddick OJ, O'Brien JM, Wattam-Bell J, Atkinson J, Turner R (2000) Form and motion coherence activate independent, but not dorsal/ventral segregated, networks in the human brain. Curr Biol 10(12):731–734

Bradley DC, Chang GC, Andersen RA (1998) Encoding of three-dimensional structure-from-motion by primate area MT neurons. Nature 392(6677):714–717. doi:10.1038/33688

Brouwer GJ, van Ee R (2007) Visual cortex allows prediction of perceptual states during ambiguous structure-from-motion. J Neurosci 27(5):1015–1023. doi:10.1523/JNEUROSCI.4593-06.2007

Brunet D, Murray MM, Michel CM (2011) Spatiotemporal analysis of multichannel EEG: CARTOOL. Comput Intell Neurosci 2011:813870. doi:10.1155/2011/813870

Bullier J (2001) Integrated model of visual processing. Brain Res Brain Res Rev 36(2–3):96–107

Castelo-Branco M, Mendes M, Silva MF, Januario C, Machado E, Pinto A, Figueiredo P, Freire A (2006) Specific retinotopically based magnocellular impairment in a patient with medial visual dorsal stream damage. Neuropsychologia 44(2):238–253. doi:10.1016/j.neuropsychologia.2005.05.005

Cottereau BR, McKee SP, Norcia AM (2014) Dynamics and cortical distribution of neural responses to 2D and 3D motion in human. J Neurophysiol 111(3):533–543. doi:10.1152/jn.00549.2013

Cowey A, Vaina LM (2000) Blindness to form from motion despite intact static form perception and motion detection. Neuropsychologia 38(5):566–578

de Jong BM, Shipp S, Skidmore B, Frackowiak RS, Zeki S (1994) The cerebral activity related to the visual perception of forward motion in depth. Brain 117(Pt 5):1039–1054

Dodd JV, Krug K, Cumming BG, Parker AJ (2001) Perceptually bistable three-dimensional figures evoke high choice probabilities in cortical area MT. J Neurosci 21(13):4809–4821

Dupont P, Orban GA, De Bruyn B, Verbruggen A, Mortelmans L (1994) Many areas in the human brain respond to visual motion. J Neurophysiol 72(3):1420–1424

Dupont P, De Bruyn B, Vandenberghe R, Rosier AM, Michiels J, Marchal G, Mortelmans L, Orban GA (1997) The kinetic occipital region in human visual cortex. Cereb Cortex 7(3):283–292

Fattori P, Pitzalis S, Galletti C (2009) The cortical visual area V6 in macaque and human brains. J Physiol Paris 103(1–2):88–97. doi:10.1016/j.jphysparis.2009.05.012

Ferber S, Humphrey GK, Vilis T (2003) The lateral occipital complex subserves the perceptual persistence of motion-defined groupings. Cereb Cortex 13(7):716–721

Galletti C, Fattori P (2003) Neuronal mechanisms for detection of motion in the field of view. Neuropsychologia 41(13): 1717–1727

Gilaie-Dotan S (2015) Which visual functions depend on intermediate visual regions? Insights from a case of developmental visual form agnosia. Neuropsychologia. doi:10.1016/j.neuropsychologia.2015.07.023

Gilaie-Dotan S, Bentin S, Harel M, Rees G, Saygin AP (2011) Normal form from biological motion despite impaired ventral stream function. Neuropsychologia 49(5):1033–1043. doi:10.1016/j.neuropsychologia.2011.01.009

Gilaie-Dotan S, Saygin AP, Lorenzi LJ, Egan R, Rees G, Behrmann M (2013) The role of human ventral visual cortex in motion perception. Brain 136(Pt 9):2784–2798. doi:10.1093/brain/awt214

Goebel R, Khorram-Sefat D, Muckli L, Hacker H, Singer W (1998) The constructive nature of vision: direct evidence from functional magnetic resonance imaging studies of apparent motion and motion imagery. Eur J Neurosci 10(5):1563–1573

Gonzalez Andino SL, de Peralta Grave, Menendez R, Lantz CM, Blank O, Michel CM, Landis T (2001) Non-stationary distributed source approximation: an alternative to improve localization procedures. Hum Brain Mapp 14(2):81–95

Goodale MA, Milner AD (1992) Separate visual pathways for perception and action. Trends Neurosci 15(1):20–25

Grave de Peralta Menendez R, Murray MM, Michel CM, Martuzzi R, Gonzalez Andino SL (2004) Electrical neuroimaging based on biophysical constraints. Neuroimage 21(2):527–539

Grill-Spector K, Kushnir T, Edelman S, Itzchak Y, Malach R (1998) Cue-invariant activation in object-related areas of the human occipital lobe. Neuron 21(1):191–202

Grunewald A, Bradley DC, Andersen RA (2002) Neural correlates of structure-from-motion perception in macaque V1 and MT. J Neurosci 22(14):6195–6207

Gulyas B, Heywood CA, Popplewell DA, Roland PE, Cowey A (1994) Visual form discrimination from color or motion cues: functional anatomy by positron emission tomography. Proc Natl Acad Sci USA 91(21):9965–9969

Heinrich SP (2007) A primer on motion visual evoked potentials. Doc Ophthalmol 114(2):83–105

Jiang Y, Boehler CN, Nonnig N, Duzel E, Hopf JM, Heinze HJ, Schoenfeld MA (2008) Binding 3-D object perception in the human visual cortex. J Cogn Neurosci 20(4):553–562. doi:10.1162/jocn.2008.20050

Kuba M, Kubova Z, Kremlacek J, Langrova J (2007) Motion-onset VEPs: characteristics, methods, and diagnostic use. Vision Res 47(2):189–202

Lehmann D, Ozaki H, Pal I (1987) EEG alpha map series: brain micro-states by space-oriented adaptive segmentation. Electroencephalogr Clin Neurophysiol 67(3):271–288

Lopez C, Mercier MR, Halje P, Blanke O (2011) Spatiotemporal dynamics of visual vertical judgments: early and late brain mechanisms as revealed by high-density electrical neuroimaging. Neuroscience 181:134–149. doi:10.1016/j.neuroscience.2011.02.009

Losey F, Safran AB, Mermound C, Michel C, Landis T (1998) Visual perception of movement. A normative study. Klin Monbl Augenheilkd 212(5):379–381. doi:10.1055/s-2008-1034911

Malach R, Reppas JB, Benson RR, Kwong KK, Jiang H, Kennedy WA, Ledden PJ, Brady TJ, Rosen BR, Tootell RB (1995) Object-related activity revealed by functional magnetic resonance imaging in human occipital cortex. Proc Natl Acad Sci USA 92(18):8135–8139

Matheson HE, McMullen PA (2010) Neuropsychological dissociations between motion and form perception suggest functional organization in extrastriate cortical regions in the human brain. Brain Cogn 74(2):160–168. doi:10.1016/j.bandc.2010.07.009

Maunsell JH, Newsome WT (1987) Visual processing in monkey extrastriate cortex. Annu Rev Neurosci 10:363–401. doi:10.1146/annurev.ne.10.030187.002051

Mercier M, Schwartz S, Michel CM, Blanke O (2009) Motion direction tuning in human visual cortex. Eur J Neurosci 29(2):424–434. doi:10.1111/j.1460-9568.2008.06583.x

Michel CM, Murray MM (2012) Towards the utilization of EEG as a brain imaging tool. Neuroimage 61(2):371–385. doi:10.1016/j.neuroimage.2011.12.039

Michel CM, Grave de Peralta R, Lantz G, Gonzalez Andino S, Spinelli L, Blanke O, Landis T, Seeck M (1999) Spatiotemporal EEG analysis and distributed source estimation in presurgical epilepsy evaluation. J Clin Neurophysiol 16(3):239–266

Michel CM, Thut G, Morand S, Khateb A, Pegna AJ, Grave de Peralta R, Gonzalez S, Seeck M, Landis T (2001) Electric source imaging of human brain functions. Brain Res Brain Res Rev 36(2–3):108–118

Mishkin M, Ungerleider LG (1982) Contribution of striate inputs to the visuospatial functions of parieto-preoccipital cortex in monkeys. Behav Brain Res 6(1):57–77

Murray SO, Olshausen BA, Woods DL (2003) Processing shape, motion and three-dimensional shape-from-motion in the human cortex. Cereb Cortex 13(5):508–516

Murray MM, Brunet D, Michel CM (2008) Topographic ERP analyses: a step-by-step tutorial review. Brain Topogr 20(4):249–264

Niedeggen M, Wist ER (1999) Characteristics of visual evoked potentials generated by motion coherence onset. Brain Res Cogn Brain Res 8(2):95–105

Orban GA, Sunaert S, Todd JT, Van Hecke P, Marchal G (1999) Human cortical regions involved in extracting depth from motion. Neuron 24(4):929–940

Paradis AL, Cornilleau-Peres V, Droulez J, Van De Moortele PF, Lobel E, Berthoz A, Le Bihan D, Poline JB (2000) Visual perception of motion and 3-D structure from motion: an fMRI study. Cereb Cortex 10(8):772–783

Pascual-Marqui RD, Michel CM, Lehmann D (1995) Segmentation of brain electrical activity into microstates: model estimation and validation. IEEE Trans Biomed Eng 42(7):658–665

Peuskens H, Claeys KG, Todd JT, Norman JF, Van Hecke P, Orban GA (2004) Attention to 3-D shape, 3-D motion, and texture in 3-D structure from motion displays. J Cogn Neurosci 16(4):665–682. doi:10.1162/089892904323057371

Pitzalis S, Galletti C, Huang RS, Patria F, Committeri G, Galati G, Fattori P, Sereno MI (2006) Wide-field retinotopy defines human cortical visual area v6. J Neurosci 26(30):7962–7973. doi:10.1523/JNEUROSCI.0178-06.2006

Pitzalis S, Sereno MI, Committeri G, Fattori P, Galati G, Patria F, Galletti C (2010) Human v6: the medial motion area. Cereb Cortex 20(2):411–424. doi:10.1093/cercor/bhp112

Pitzalis S, Sdoia S, Bultrini A, Committeri G, Di Russo F, Fattori P, Galletti C, Galati G (2013) Selectivity to translational egomotion

in human brain motion areas. PLoS One 8(4):e60241. doi:10.1371/journal.pone.0060241

Plomp G, Mercier MR, Otto TU, Blanke O, Herzog MH (2009) Non-retinotopic feature integration decreases response-locked brain activity as revealed by electrical neuroimaging. Neuroimage 48(2):405–414. doi:10.1016/j.neuroimage.2009.06.031

Regan D, Giaschi D, Sharpe JA, Hong XH (1992) Visual processing of motion-defined form: selective failure in patients with parietotemporal lesions. J Neurosci 12(6):2198–2210

Schenk T, Zihl J (1997) Visual motion perception after brain damage: II. Deficits in form-from-motion perception. Neuropsychologia 35(9):1299–1310

Schoenfeld MA, Woldorff M, Duzel E, Scheich H, Heinze HJ, Mangun GR (2003) Form-from-motion: MEG evidence for time course and processing sequence. J Cogn Neurosci 15(2):157–172. doi:10.1162/089892903321208105

Self MW, Zeki S (2005) The integration of colour and motion by the human visual brain. Cereb Cortex 15(8):1270–1279. doi:10.1093/cercor/bhi010

Spinelli L, Andino SG, Lantz G, Seeck M, Michel CM (2000) Electromagnetic inverse solutions in anatomically constrained spherical head models. Brain Topogr 13(2):115–125

Sunaert S, Van Hecke P, Marchal G, Orban GA (1999) Motion-responsive regions of the human brain. Exp Brain Res 127(4):355–370

Thirioux B, Mercier MR, Jorland G, Berthoz A, Blanke O (2010) Mental imagery of self-location during spontaneous and active self-other interactions: an electrical neuroimaging study. J Neurosci 30(21):7202–7214. doi:10.1523/JNEUROSCI.3403-09.2010

Thirioux B, Mercier MR, Blanke O, Berthoz A (2014) The cognitive and neural time course of empathy and sympathy: an electrical neuroimaging study on self-other interaction. Neuroscience 267:286–306. doi:10.1016/j.neuroscience.2014.02.024

Tononi G, Sporns O, Edelman GM (1992) Reentry and the problem of integrating multiple cortical areas: simulation of dynamic integration in the visual system. Cereb Cortex 2(4):310–335

Tootell RB, Taylor JB (1995) Anatomical evidence for MT and additional cortical visual areas in humans. Cereb Cortex 5(1):39–55

Tootell RB, Reppas JB, Kwong KK, Malach R, Born RT, Brady TJ, Rosen BR, Belliveau JW (1995) Functional analysis of human MT and related visual cortical areas using magnetic resonance imaging. J Neurosci 15(4):3215–3230

Tootell RB, Dale AM, Sereno MI, Malach R (1996) New images from human visual cortex. Trends Neurosci 19(11):481–489

Ungerleider LG, Haxby JV (1994) 'What' and 'where' in the human brain. Curr Opin Neurobiol 4(2):157–165

Vaina LM (1989) Selective impairment of visual motion interpretation following lesions of the right occipito-parietal area in humans. Biol Cybern 61(5):347–359

Vaina LM, Gross CG (2004) Perceptual deficits in patients with impaired recognition of biological motion after temporal lobe lesions. Proc Natl Acad Sci USA 101(48):16947–16951. doi:10.1073/pnas.0407668101

Vaina LM, Soloviev S, Bienfang DC, Cowey A (2000) A lesion of cortical area V2 selectively impairs the perception of the direction of first-order visual motion. Neuroreport 11(5):1039–1044

Vaina LM, Sikoglu EM, Soloviev S, LeMay M, Squatrito S, Pandiani G, Cowey A (2010) Functional and anatomical profile of visual motion impairments in stroke patients correlate with fMRI in normal subjects. J Neuropsychol 4(Pt 2):121–145. doi:10.1348/174866409X471760

Vanduffel W, Fize D, Peuskens H, Denys K, Sunaert S, Todd JT, Orban GA (2002) Extracting 3D from motion: differences in human and monkey intraparietal cortex. Science 298(5592):413–415. doi:10.1126/science.1073574

Wang J, Zhou T, Qiu M, Du A, Cai K, Wang Z, Zhou C, Meng M, Zhuo Y, Fan S, Chen L (1999) Relationship between ventral stream for object vision and dorsal stream for spatial vision: an fMRI + ERP study. Hum Brain Mapp 8(4):170–181. doi:10.1002/(SICI)1097-0193(1999)8:4<170:AID-HBM2>3.0.CO;2-W

Watson JD, Myers R, Frackowiak RS, Hajnal JV, Woods RP, Mazziotta JC, Shipp S, Zeki S (1993) Area V5 of the human brain: evidence from a combined study using positron emission tomography and magnetic resonance imaging. Cereb Cortex 3(2):79–94

Zhuang J, Peltier S, He S, LaConte S, Hu X (2008) Mapping the connectivity with structural equation modeling in an fMRI study of shape-from-motion task. Neuroimage 42(2):799–806. doi:10.1016/j.neuroimage.2008.05.036